ACS OMEGA

Open Access

This article is licensed under CC-BY-NC-ND 4.0

http://pubs.acs.org/journal/acsodf

Article

Predicting Poisson's Ratio: A Study of Semisupervised Anomaly Detection and Supervised Approaches

Raheel Hammad* and Sownyak Mondal*

Cite This: *ACS Omega* 2024, 9, 1956−1961

Read Online

ACCESS | Metrics & More | Article Recommendations | Supporting Information

ABSTRACT: Auxetics are a rare class of materials that exhibit a negative Poisson's ratio. The existence of these auxetic materials is rare but has a large number of applications in the design of exotic materials. We build a complete machine learning framework to detect Auxetic materials as well as Poisson's ratio of non-auxetic materials. A semisupervised anomaly detection model is presented, which is capable of separating out the auxetics materials (treated as an anomaly) from an unknown database with an average precision of 0.64. Another regression model (supervised) is also created to predict the Poisson's ratio of non-auxetic materials with an R^2 of 0.82. Additionally, this regression model helps us to find the optimal features for the anomaly detection model. This methodology can be generalized and used to discover materials with rare physical properties.

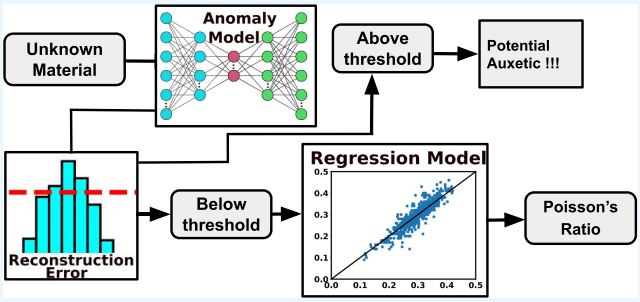

INTRODUCTION

As a fundamental elastic property, Poisson's ratio reflects the ratio of lateral strain to the axial strain under an applied stress.[1] It governs the distribution of the stress and strain fields as well as the deformation process of a material. Poisson's ratio also affects the speed of wave in material. For example, if the value is large, the longitudinal wave propagates much faster than shear wave and vice versa.[2] In seismology, it is employed to analyze rock properties and forecast the propagation of seismic waves in the Earth's crust. In the realm of the theory of elasticity, it is acceptable to have materials exhibiting a negative Poisson's ratio (NPR). Counterintuitively, these exotic NPR materials contract under applied tension.[3] They are termed as "Auxetic" materials. The auxeticity of these materials leads to many special properties like enhancement of plane strain fracture resistance, increment of fracture toughness, shear modulus, and even boosting of acoustic response.[4]

Several 2D materials, including graphene oxide, transition metal selenides, and transition metal halides with the stoichiometry MX (where M represents elements such as V, Cr, Mn, and Fe; X represents elements like Se, Cl, Br, and I), exhibit auxetic behavior.[5,6] Although most auxetic materials with homogeneous (NPR for all directions) values are either porous foams or specifically designed meta-materials,[7−9] Dagdelen et al.[10] came up with three distinctive types of auxetic crystals and discovered some new auxetic compounds. Later, Chibani et al.[11] reported a few more auxetic materials.

In recent years, the substantial data generated through computational and experimental methods, along with the application of advanced machine learning (ML) techniques, has propelled the field of materials science into a new era often described as the fourth paradigm of scientific exploration.[12] Different machine learning (ML) algorithms are utilized to generate efficient and accurate predictions of elastic properties of materials like Young's modulus and shear modulus.[13] Typically, supervised algorithms are used to build accurate models where the model is trained using a fully labeled data set. The prediction is then done by minimizing the error metric in both sets of problems, classifications and regressions. Bulk and shear moduli have been predicted with great accuracy in search of superhard materials in these reports.[14−17] Deng et al.[18] explained the difficulties of building an ML model to predict Poisson's ratio with high accuracy but still managed to achieve R^2 around 0.7 by Random Forest Regression (RFR) for a class of materials called oxide glass. Gaillac et al.[19] described how important a supervised ML model can be to speed up the discovery of auxetic zeolite materials. Poisson's ratio is predicted for specific binary alloys also using supervised ML.[20] So far, the literature is missing an ML model that can predict Poisson's ratio with good accuracy for any general material.

On the other hand, applications of anomaly detection algorithms have increased rapidly to address real-world issues like fraud detection in banks,[21,22] cyber threats,[23] and disease variant detection.[24] Historically, many of these algorithms were

Received: November 7, 2023
Revised: November 22, 2023
Accepted: December 13, 2023
Published: December 29, 2023

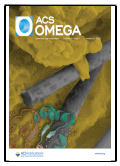

© 2023 The Authors. Published by American Chemical Society

designed to find outliers to be removed. In a recent report, Zhang et al. introduced an anomaly detection model to the material community for the first time.[25] The fact that the radial distribution function is poorly reconstructed for superhard materials is the basis for their unsupervised anomaly detection model. In a recent article, Schrier et al.[26] proposed how ML can be utilized to get the exceptions and anomalies that exist in chemical and material science.

In this study, we aim to build a general model using supervised ML algorithms to predict Poisson's ratio. We observe that the accuracy varies drastically based on whether the auxetics materials are used in the data set or not. Moreover, the presence of homogeneous auxetic material in nature is pretty low. So we treat the NPR materials as anomalies. Therefore, we build an Autoencoder Neural Network (ANN)-based semisupervised anomaly detection model where labeled data is used to train the Autoencoder. Materials with only a positive Poisson's ratio are used for training so that the autoencoder fails to reconstruct the auxetic materials. Based on the reconstruction loss, we can identify our anomalies, the NPR materials. We show that the precision of this anomaly detection model is 0.64 with an F_1score of 0.57. We also build a supervised regression model to predict Poisson's ratio with an R^2 of 0.82 applicable to general non-auxetic materials. The supervised model is used to determine the optimal descriptors for learning the pattern of Poisson's ratio. This in turn helps in optimizing both the supervised and anomalous detection models.

METHODS

We investigated several semisupervised anomaly detection methods like One Class SVM,[27] Isolation forest,[28] and Autoencoder.[29] In all of these methods, a score is associated with each data point, which is then used to label the point as anomaly or normal class. We have observed that Autoencoder works best for our system. The details about anomaly detection using One class SVM and isolation forest are given in the Supporting Information.

The choice of the evaluation metric plays an important role in ML problems. Anomaly detection is no different. In fact, more so since using a commonly used classification metric like accuracy might be counterproductive given the large imbalance of data sets for anomaly detection. Therefore, we use F_1 score and Precision for our model; formulas for the same are given below.

$$\text{precision} = \frac{\text{TP}}{\text{TP} + \text{FP}} \tag{1}$$

$$\text{recall} = \frac{\text{TP}}{\text{TP} + \text{FN}} \tag{2}$$

$$F_1 = \frac{2 \times \text{precision} \times \text{recall}}{\text{precision} + \text{recall}} \tag{3}$$

where TP, TN, FP, and FN stand for true positive, true negative, false positive, and false negative, respectively. Multiple incorrect identifications leading to false positives contribute to reduced precision, while failing to identify true positives results in a decreased recall. The F_1 score serves as a means to strike a balance between these two metrics and is consequently employed for the purpose of optimizing the hyperparameters of the Autoencoder.

The ANN Autoencoder is shown in Figure 1. The left side (encoder) of the network encodes the input data X into a latent dimension (central layer), while the right side (decoder) of the network aims to reconstruct the input X′. In an ideal scenario, the input passed through the Autoencoder is perfectly reconstructed (X = X′). However, information is lost during the encoding and decoding process. This results in different X and X′, using which a reconstruction error is calculated. This reconstruction error is the anomaly score that we discussed earlier. It reveals how the data are represented in the latent layers and are widely used for pattern recognition.

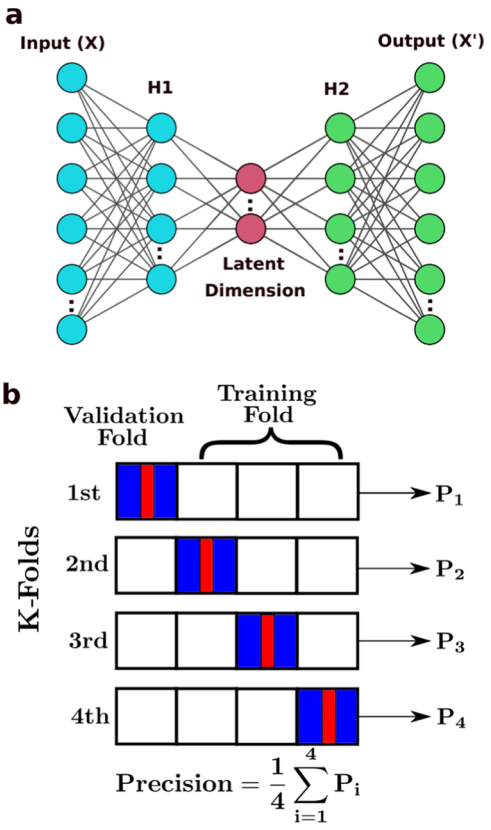

Figure 1. (a) Schematic of the Autoencoder used in the semisupervised anomaly detection. (b) K-Fold cross-validation used in the Anomaly model. Auxetic Materials (red strip) are constrained to be kept in all of the validation folds. P_i denotes the precision in each fold.

The autoencoder is trained using a combination of crystal and elemental properties. These elemental descriptors are represented using the mathematical expressions average, minimum, maximum, and difference, respectively. Out of the total 170 features, we ended up taking 60 features.

The process of choosing the features is described in the Results and Discussion section. These 60 descriptors are provided as input to the Autoencoder in Figure 1, which compresses it to the latent dimension using 2 fully connected hidden layers. The ReLU (Rectified Linear Unit) activation function is applied at each synaptic connection to introduce nonlinear properties within the neural network. The decoder network uses a ReLU for the hidden layer and a sigmoid for the output layer. The autoencoder network is trained to minimize the loss using ADAM,[30] a stochastic gradient descent method. The loss in this case is defined as the mean squared error between input X and output X′. Usually, the network is optimized by minimizing this loss to obtain better reconstructions of the input. However, for Anomaly detection, this is not necessary; therefore, we optimize the hyperparameters and the

https://doi.org/10.1021/acsomega.3c08861
ACS Omega 2024, 9, 1956−1961

network architecture by maximizing the F_1 score (see the Supporting Information for details).

Supervised Regression Model. We have employed Support Vector Regression (SVR), RFR, and Gradient Boosting Regression (GBR) to predict the Poisson's ratio of non-auxetic materials using supervised learning. The models were trained on the previously mentioned descriptors using 80% percent of the set, while 20% of the set was reserved for testing. The coefficients of determination (R^2) and root mean squared error (RMSE) were used to validate the models. The formulas for the same are given below.

$$R^2 = 1 - \frac{\sum_i \left(y_i - \hat{y}_i\right)^2}{\sum_i \left(y_i - \overline{y}\right)^2} \tag{4}$$

$$\mathrm{RMSE} = \sqrt{\frac{\sum_i \left(y_i - \hat{y}_i\right)^2}{n}} \tag{5}$$

where $\overline{y}$ represents the average true value, y_i signifies the ith true value, $\hat{y}_i$ denotes the ith predicted value, and n is the count of samples. As R^2 approaches 1 and RMSE diminishes toward 0, the model's predictions converge closer to the values computed using DFT.

Data Processing. In a recent report, Chibani et al.[11] explored the mechanical properties of more than 13k materials. After collecting the elastic tensor data from Materials Project, properties like shear modulus, bulk modulus, Young's modulus, Poisson's ratio, and linear compressibility have been calculated using Elate software developed by the same group. They reported 121 auxetic materials (average Poisson's ratio is negative) out of 11 764 materials. However, only 75 materials out of them are stable. Only stable auxetic materials are used in this study. All of the necessary descriptors of these materials have been gathered from the ever-reliable Material Project. To ensure that the Autoencoder model shown in Figure 1 learns the desired patterns effectively, the anomaly model should consider only the auxetic materials as exceptions. Hence, we clean the data based on the widely used protocol of removing points below Q1 − 1.5 × IQR (Interquartile range) or above Q3 + 1.5 × IQR of the features, where Q1, Q3, and IQR are 25th percentile, 75th percentile, and Q3−Q1 respectively. Additionally cleaning the data using this method helps in increasing the accuracy of the regression model. This has been shown in detail in the Supervised Regression Model section.

For example, materials with energy above the convex hull less than 80 meV (stability criteria) are retained. Moreover, substances having lower than 46 computationally traceable sites are kept.[10] More details of the cleaning are provided at https://github.com/Sudo-Raheel/Poisson_ratio. The reduced set containing 15 auxetic materials and 4476 normal samples with 60 descriptors (discussed later) is fed into the model.

RESULTS AND DISCUSSION

Previous studies[11] suggest that roughly 1% of the total materials are auxetic in nature. Due to the extremely skewed nature of the distribution, we treat auxetic materials as anomalies. To this end, we develop a semisupervised anomaly detection to predict the auxeticity of material.

Although unsupervised anomaly detection techniques are widely used, it is a challenging task to connect to a targeted quantity using unlabeled data. As shown by Brogch et al.,[25] the MRBT crystal features used in the study correctly label (poorly reconstructed) the Superhard materials as anomalies. In our case, we want the features to be poorly reconstructed for auxetic materials. Therefore, in an unsupervised model, the only parameters that can be tuned are the features and the network architecture since there is no target quantity to fit, unlike supervised learning. Therefore, finding the optimal set of features and network architecture that will best represent the target quantity can be a daunting task. To ease this, we employ a semisupervised learning approach in the sense that during the training of the Autoencoder, it is only fed with normal class (non-auxetic) samples in the hope that it learns the patterns related to the normal class in a better way. This would result in the auxetic materials being reconstructed poorly, and thereby distinguishing them will be easier.[31]

We used 4-fold validation to confirm that the model performs equally well on the total data, thereby minimizing the risk of overfitting. Moreover, at each fold, the auxetic materials are kept in the testing set only. Since it has been already discussed that the model will be trained on the normal class only.

4-Fold validation additionally mimics the realistic auxetics percentage in nature; this has been discussed in detail in the Supporting Information (Figure S2). On top of this, we shuffle the data twice and repeat the 4-fold validation to make the metrics more robust.

The model can separate the auxetic materials from the rest with an average F_1 score of 0.57 and an average Precision of 0.64 over the full set. The model labels materials above a certain threshold of reconstruction error as anomalies. This threshold is decided by maximizing the F_1 score. The hyperparameters and the architecture of the autoencoder are also optimized by maximizing the F_1 score over multiple folds (see the Supporting Information for details).

Figure 2 shows that the model labels 8 out of 15 auxetic as Anomalies, while only 5 out of 1119 non-auxetic are incorrectly

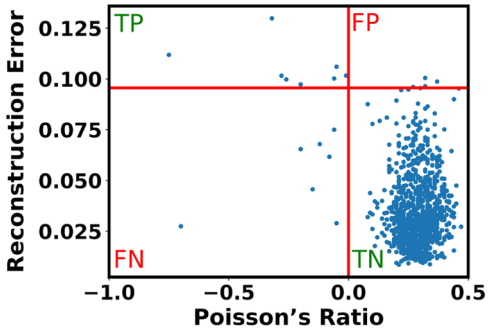

Figure 2. Truth table plot of reconstruction error vs Poisson's ratio for semisupervised anomaly detection model using Autoencoder.

labeled as Anomalies. The threshold for labeling anomalies is approximately 99 percentile of the total reconstruction error for the testing case. The model successfully labels all of the α-cristobalite SiO_2 materials as anomalies, which are well-known auxetics.[32]

Additionally, we make separate sets of material with high reconstruction error(above 90 percentile) and low reconstruction. This is done to signify the features that are being reconstructed poorly in the materials labeled as potential anomalies.

If a property is reconstructed properly, both histograms should be overlapped; if not, there should be a clear separation

https://doi.org/10.1021/acsomega.3c08861
ACS Omega 2024, 9, 1956−1961

between the two sets. We found that average d-valence electrons and average density are not reconstructed properly for the high reconstruction error set (Figure 3). Many features are

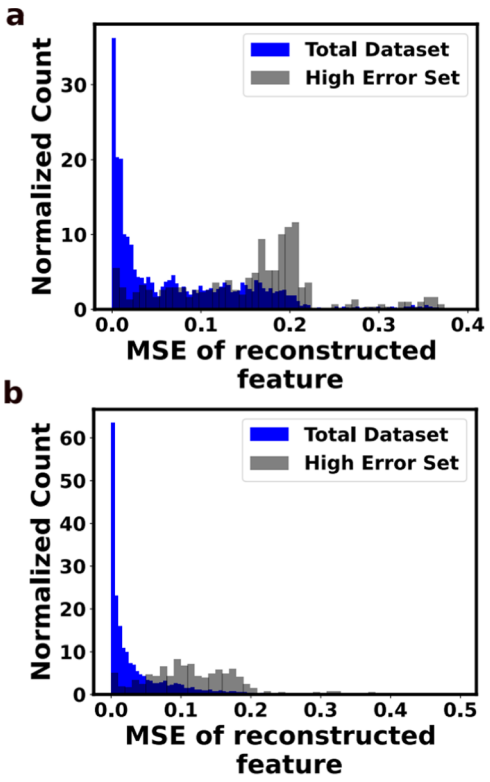

Figure 3. Distribution of the individual reconstruction error for the descriptors: (a) average valence d and (b) average Density.

reconstructed well throughout the whole region (Figure S3). Interestingly, it is well known that density and valence electrons are important properties for predicting Poisson's ratio[33] (Figure S4). Moreover, these quantities have a good correlation with the Poisson's ratio as shown in Figure 5 (Figure S7 also). This further validates that the autoencoder is learning the pattern of positive Poisson's ratio.

Supervised Model. The regression model is built to predict the values of non-auxetic Poisson's ratio. However, predicting Poisson's ratio for a general material has turned out to be a difficult task. This is due to the noisy nature of Poisson's ratio data sets.[16,18] Cleaning of the data set is done as mentioned in the Data Processing section. Table 1 shows the performance of

Table 1. Comparison of Regression (GBR) Model Performance for Clean and Raw Dataset

data set	training data R^2	testing data R^2
cleaned	0.999	0.821
raw	0.969	0.506

GBR on training and testing sets for both types of data(raw and cleaned) using the same features. It shows that the model fails to generalize on the testing(raw) set, which indicates overfitting.

While the improved performance on the testing (cleaned) set shows that IQR cleaning decreases the noise in the data set.

The cleaned data set is fed into various different algorithms, namely, GBR, SVR, RFR, CatBoost, LGBM, and NN. The results are shown in Figures 4a and S5; Gradient Boosting is performing the best. We obtain an MAE of 0.019 and R^2 of 0.82 in predicting the Poisson's ratio for non-auxetic materials.

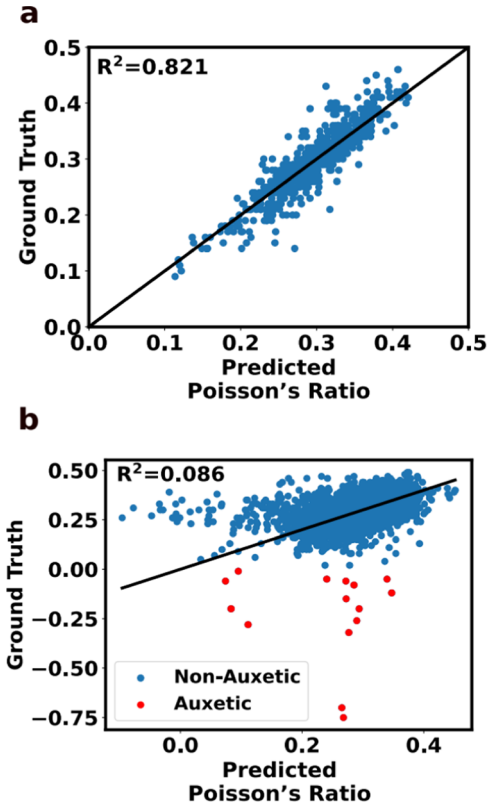

Figure 4. Gradient Boosting predicted values vs the ground truth values reported in Materials Project: (a) for non-auxetic data set and (b) for total data set (auxetic + non-auxetic).

In Figure S4, we have shown the importance scores for the different features using RFR. Among the structural variables, the average crystal radius and minimum bond seem to be affecting the Poisson's ratio, while electronic counts like average s,p,d valence electrons and total valence electron count play an important role in the model. This is verified by the Pearson correlation plot between the Poisson's ratio and other important features in Figure 5. The features were sorted according to importance scores by RFR (Figure S4). Afterward, we maximized the cross-validated R^2 score to choose the optimal number of features, which turns out to be 60. Figure S6 shows the Pearson correlation heat map for the 60 features used in the model. The low inner correlations between features indicate the low redundancy between features In addition to this, the good correlation with the ground truth values dictates that these features are optimal for predicting the Poisson's ratio.

Using the same features, we use GBR to model the Poisson's ratio for the data set used in the anomaly detection method. We used 4-fold validation to train and test the total data set, and the results are shown in Figure 4b. Including the auxetic materials deteriorates the performance of the model, especially in predicting the auxetic materials itself. This further justifies the treatment of auxetic materials as anomalies. Additionally, this plot proves that the features are optimal for learning Poisson's ratio pattern for non-auxetic materials. Therefore, a similar feature set was used for training the autoencoders for anomaly detection.

https://doi.org/10.1021/acsomega.3c08861
ACS Omega 2024, 9, 1956−1961

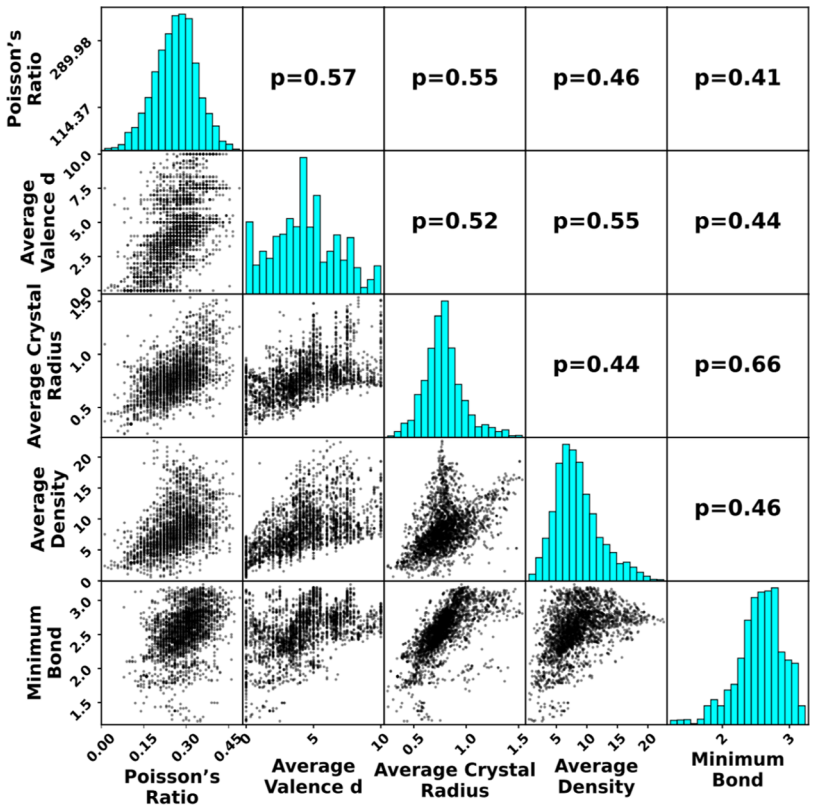

Figure 5. Pearson correlation scatter matrix for target variable (Poisson's ratio) and few important features.

CONCLUSIONS

To date, in the material science literature, mostly various kinds of supervised models have been developed to predict different properties. These approaches fail to predict exotic properties due to a lack of data. In this work, we have demonstrated a new methodology where a semisupervised anomaly detection algorithm is used to predict the auxetic materials despite a severe lack of data on auxetic materials. Moreover, a regression model is built to predict the Poisson's ratio for non-auxetic material. This model also helps in determining the optimal features for learning the Poisson's ratio, which in turn helps in building the descriptors for anomaly detection. Therefore, we present a general framework to predict the poisson's ratio as shown in Figure 6. This complete framework exhibits versatility, as it can be applied to the prediction of various material properties beyond Poisson's ratio. Particularly, it is well suited for properties that exhibit both rare and normal regimes, such as negative and positive refractive indices.

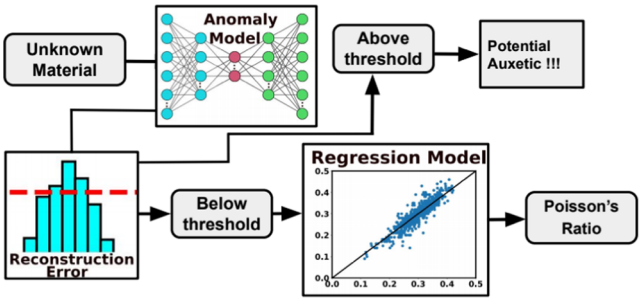

Figure 6. Schematic of how both the models can be utilized to get the Poisson's ratio of an unknown material.

ASSOCIATED CONTENT

Data Availability Statement

All of the data and code used in the work are kept here https://github.com/Sudo-Raheel/Poisson_ratio and will be made public once the manuscript is accepted.

Supporting Information

The Supporting Information is available free of charge at https://pubs.acs.org/doi/10.1021/acsomega.3c08861.

Results of two other anomaly detection models, namely, Isolation Forest and One Class SVM; importance scores of the features using Random Forest; a table highlighting important results and another with hyperparameters of two models (PDF)

AUTHOR INFORMATION

Corresponding Authors

Raheel Hammad − *Tata Institute of Fundamental Research Hyderabad, Hyderabad 500046 Telangana, India*; Email: raheelhammad@tifrh.res.in

Sownyak Mondal − *Tata Institute of Fundamental Research Hyderabad, Hyderabad 500046 Telangana, India*; orcid.org/0009-0002-4470-1995; Email: msownyak@tifrh.res.in

Complete contact information is available at: https://pubs.acs.org/10.1021/acsomega.3c08861

Notes

The authors declare no competing financial interest.

https://doi.org/10.1021/acsomega.3c08861
ACS Omega 2024, 9, 1956−1961

■ ACKNOWLEDGMENTS

The authors thank Prof. Soumya Ghosh for the computing facility and the critical comments on the manuscript. They also thank Chandrashekhar Iyer and M. Sahil for useful discussions. We also want to acknowledge TIFR Hyderabad for funding and facilities.

■ REFERENCES

(1) Ledbetter, H. M.; Reed, R. P. Elastic Properties of Metals and Alloys, I. Iron, Nickel, and Iron-Nickel Alloys. *J. Phys. Chem. Ref. Data* **1973**, *2* (3), 531−618.
(2) Lakes, R. S. Negative-Poisson's-Ratio Materials: Auxetic Solids. *Annu. Rev. Mater. Res.* **2017**, *47* (1), 63−81.
(3) Evans, K. E.; Nkansah, M. A.; Hutchinson, I. J.; Rogers, S. C. Molecular Network Design. *Nature* **1991**, *353* (6340), 124.
(4) Yang, W.; Li, Z.-M.; Shi, W.; Xie, B.-H.; Yang, M.-B. Review on Auxetic Materials. *J. Mater. Sci.* **2004**, *39* (10), 3269−3279.
(5) Pan, J.; Zhang, Y.-F.; Zhang, J.; Banjade, H.; Yu, J.; Yu, L.; Du, S.; Ruzsinszky, A.; Hu, Z.; Yan, Q. Auxetic Two-Dimensional Transition Metal Selenides and Halides. *npj Comput. Mater.* **2020**, *6* (1), 154.
(6) Wan, J.; Jiang, J.-W.; Park, H. S. Negative Poisson's Ratio in Graphene Oxide. *Nanoscale* **2017**, *9* (11), 4007−4012.
(7) Evans, K. E.; Alderson, A. Auxetic Materials: Functional Materials and Structures from Lateral Thinking! *Adv. Mater.* **2000**, *12* (9), 617−628.
(8) Bhullar, S. K. Three Decades of Auxetic Polymers: A Review. *e-Polymers* **2015**, *15* (4), 205−215, DOI: 10.1515/epoly-2014-0193.
(9) Kolken, H. M. A.; Zadpoor, A. A. Auxetic Mechanical Metamaterials. *RSC Adv.* **2017**, *7* (9), 5111−5129.
(10) Dagdelen, J.; Montoya, J.; de Jong, M.; Persson, K. Computational Prediction of New Auxetic Materials. *Nat. Commun.* **2017**, *8* (1), No. 323.
(11) Chibani, S.; Coudert, F.-X. Systematic Exploration of the Mechanical Properties of 13 621 Inorganic Compounds. *Chem. Sci.* **2019**, *10* (37), 8589−8599.
(12) Wang, Z.; Sun, Z.; Yin, H.; Liu, X.; Wang, J.; Zhao, H.; Pang, C. H.; Wu, T.; Li, S.; Yin, Z.; Yu, X.-F. Data-Driven Materials Innovation and Applications. *Adv. Mater.* **2022**, *34* (36), No. 2104113.
(13) Chibani, S.; Coudert, F.-X. Machine Learning Approaches for the Prediction of Materials Properties. *APL Mater.* **2020**, *8* (8), No. 080701.
(14) Tehrani, A. M.; Oliynyk, A. O.; Parry, M.; Rizvi, Z.; Couper, S.; Lin, F.; Miyagi, L.; Sparks, T. D.; Brgoch, J. Machine Learning Directed Search for Ultraincompressible, Superhard Materials. *J. Am. Chem. Soc.* **2018**, *140* (31), 9844−9853.
(15) Avery, P.; Wang, X.; Oses, C.; Gossett, E.; Proserpio, D. M.; Toher, C.; Curtarolo, S.; Zurek, E. Predicting Superhard Materials via a Machine Learning Informed Evolutionary Structure Search. *npj Comput. Mater.* **2019**, *5* (1), 89.
(16) Mazhnik, E.; Oganov, A. R. Application of Machine Learning Methods for Predicting New Superhard Materials. *J. Appl. Phys.* **2020**, *128* (7), No. 075102.
(17) Zhang, Z.; Tehrani, A. M.; Oliynyk, A. O.; Day, B.; Brgoch, J. Finding the Next Superhard Material through Ensemble Learning. *Adv. Mater.* **2021**, *33* (5), No. 2005112.
(18) Deng, B. Machine Learning on Density and Elastic Property of Oxide Glasses Driven by Large Dataset. *J. Non-Cryst. Solids* **2020**, *529*, No. 119768.
(19) Gaillac, R.; Chibani, S.; Coudert, F.-X. Speeding Up Discovery of Auxetic Zeolite Frameworks by Machine Learning. *Chem. Mater.* **2020**, *32* (6), 2653−2663.
(20) Linton, N.; Aidhy, D. S. A Machine Learning Framework for Elastic Constants Predictions in Multi-Principal Element Alloys. *APL Mach. Learn.* **2023**, *1* (1), No. 016109.
(21) Kim, Y.; Kogan, A. Development of an Anomaly Detection Model for a Bank's Transitory Account System. *J. Inf. Syst.* **2014**, *28* (1), 145−165.
(22) Pourhabibi, T.; Ong, K.-L.; Kam, B. H.; Boo, Y. L. Fraud Detection: A Systematic Literature Review of Graph-Based Anomaly Detection Approaches. *Decis. Support Syst.* **2020**, *133*, No. 113303.
(23) Mothukuri, V.; Khare, P.; Parizi, R. M.; Pouriyeh, S.; Dehghantanha, A.; Srivastava, G. Federated-Learning-Based Anomaly Detection for IoT Security Attacks. *IEEE Internet Things J.* **2022**, *9* (4), 2545−2554.
(24) Schlegl, T.; Seeböck, P.; Waldstein, S. M.; Schmidt-Erfurth, U.; Langs, G. Unsupervised Anomaly Detection with Generative Adversarial Networks to Guide Marker Discovery. In *Information Processing in Medical Imaging*; Niethammer, M.; Styner, M.; Aylward, S.; Zhu, H.; Oguz, I.; Yap, P.-T.; Shen, D., Eds.; Springer International Publishing: Cham, 2017; pp 146−157.
(25) Zhang, Z.; Brgoch, J. Treating Superhard Materials as Anomalies. *J. Am. Chem. Soc.* **2022**, *144* (39), 18075−18080.
(26) Schrier, J.; Norquist, A. J.; Buonassisi, T.; Brgoch, J. In Pursuit of the Exceptional: Research Directions for Machine Learning in Chemical and Materials Science. *J. Am. Chem. Soc.* **2023**, *145* (40), 21699−21716.
(27) Li, K.-L.; Huang, H.-K.; Tian, S.-F.; Xu, W. In *Improving One-Class SVM for Anomaly Detection*, Proceedings of the 2003 International Conference on Machine Learning and Cybernetics, 2003; pp 3077−3081.
(28) Liu, F. T.; Ting, K. M.; Zhou, Z.-H. In *Isolation Forest*, Eighth IEEE International Conference on Data Mining, 2008; pp 413−422.
(29) Tschannen, M.; Bachem, O.; Lucic, M.Recent Advances in Autoencoder-Based Representation Learning, 2018. arXiv:1812.05069. https://doi.org/10.48550/arXiv.1812.05069.
(30) Kingma, D. P.; Adam, J. B.A Method for Stochastic Optimization, 2017. arXiv:1412.6980. https://doi.org/10.48550/arXiv.1412.6980.
(31) Minhas, M. S.; Zelek, J.Semi-Supervised Anomaly Detection Using AutoEncoders, 2020. arXiv:2001.03674. https://doi.org/10.48550/arXiv.2001.03674.
(32) Yeganeh-Haeri, A.; Weidner, D. J.; Parise, J. B. Elasticity of α-Cristobalite: A Silicon Dioxide with a Negative Poisson's Ratio. *Science* **1992**, *257* (5070), 650−652.
(33) Gilman, J. J. *Electronic Basis of the Strength of Materials*; Cambridge University Press: Cambridge, 2003.

https://doi.org/10.1021/acsomega.3c08861
ACS Omega 2024, 9, 1956−1961